

## Quantitative characterization of aqueous solutions probed by the third-harmonic generation microscopy

V. Shcheslavskiy,<sup>a</sup> G.I. Petrov,<sup>a</sup> S. Saltiel,<sup>b</sup> and V.V. Yakovlev<sup>a,\*</sup>

<sup>a</sup> Department of Physics, University of Wisconsin—Milwaukee, P.O. Box 413, Milwaukee, WI 53201, USA

<sup>b</sup> Faculty of Physics, Sofia University, Sofia, Bulgaria

Received 31 July 2003, and in revised form 15 October 2003

### Abstract

Third-harmonic microscopy is one of the emerging techniques for noninvasive microscopic imaging of biological structures. We use a novel technique for nonlinear optical material characterization and study the effect of different environment and the structural sensitivity of the third harmonic. In particular, a transformation of collagen in solution is observed for the first time using third-harmonic generation. We also study the ultimate limits of the third harmonic to detect micro- and nanoscopic features inside living cells and find that structures as small as 50 nm can be detected using the current level of technology.

© 2003 Elsevier Inc. All rights reserved.

### 1. Introduction

Multiphoton microscopy has become an important technique for the investigation of biological phenomena where three-dimensional imaging, high contrast, and high resolution is essential for understanding the biological functions of different structures (Denk et al., 1990). Over the last years there was a great deal of attention to truly noninvasive microscopic techniques based on nonlinear optical techniques (Delfino, 1978; Freund et al., 1986; Zhang et al., 1998; Peleg et al., 1999; Moreaux et al., 2001; Campagnola et al., 2002; Barad et al., 1997; Müller et al., 1998; Squier et al., 1998; Yelin and Silberberg, 1999; Duncan et al., 1982; Zumbusch et al., 1999; Potma et al., 2000). The advantage of these techniques come from a simple fact that information about cellular structure and properties does not require a foreign marker, such as a dye molecule, but is rather supplied by the molecules of interest. Since any nonlinear optical technique relies on the high intensity of the incident laser pulses, most of the signal is coming from the highly localized focal volume, providing excellent spatial resolution and discrimination against out of fo-

cus tissue. The sensitivity of nonlinear optical techniques to the structural changes in simple systems has been proven (Shen, 1996), and it is now challenged by the complexity of biological molecules.

One of the most dramatic examples is the use of the second harmonic generation for microscopic imaging. Microscopic organization of biological molecules in ordered oriented structures like collagen fibrils (Freund et al., 1986; Campagnola et al., 2002) or cellular membranes (Zhang et al., 1998; Peleg et al., 1999; Moreaux et al., 2001; Petrov et al., 2003) gives rise to coherent second harmonic generation from these structures, allowing discrimination of these structures against the rest of the living cell. Any dynamic changes in these structures are reflected in the intensity and polarization properties of the second harmonic signal.

Another interesting application of the nonlinear optical microscopy comes from the third-harmonic generation (Barad et al., 1997; Müller et al., 1998; Squier et al., 1998; Yelin and Silberberg, 1999). In a tightly focused beam no third-harmonic generation is possible for a homogeneous medium. However, if the boundary between two media lies near the focal plane of a laser beam the third-harmonic signal is rather strong and can be easily detected using photomultiplier tube (PMT) or silicon based detector. Thus, this nonlinear optical technique can be useful in identifying and visualizing

\* Corresponding author. Fax: 1-414-229-5589.

E-mail address: [yakovlev@uwm.edu](mailto:yakovlev@uwm.edu) (V.V. Yakovlev).

interfaces inside living cells (Squier et al., 1998; Yelin and Silberberg, 1999).

However, there is an important question on how much structural information can one get from these images, what kind of dynamic changes can be observed, and what type of biologically significant processes can be followed using the technique of the third-harmonic microscopy. It is also important to understand the minimal feature size, which can be detected by this technique.

Recently we have demonstrated that third-harmonic microscopy, which utilizes the properties of circular polarized light (Yakovlev and Govorkov, 2001), can provide additional information about the structural organization on the interface, i.e., distinguish interfaces with ordered structures, like cellular membranes, from the disordered ones.

In this report we describe our results on using third-harmonic generation for characterization of solutions and biological nanostructures. First, we describe a novel technique we have recently developed (Shcheslavskiy et al., 2003), which allows fast and precise characterization of colloidal solutions in terms of their third-order nonlinear optical susceptibility. Then we demonstrate the examples of using this technique for characterization of saline solution and collagen. We demonstrate experimentally for the first time the extreme sensitivity of the third harmonic to the structural changes in collagen. Finally we will discuss the ultimate resolution imaging capabilities of the third-harmonic generation microscopy.

## 2. Theory

When high intensity laser light of a frequency  $\omega$  interacts with a medium the polarization of the medium,  $\vec{P}$ , is described by the following equation (Boyd, 1992):

$$\vec{P} = \overset{\leftrightarrow}{\chi}^{(1)} \otimes \vec{E}(\omega) + \overset{\leftrightarrow}{\chi}^{(2)} \otimes \vec{E}(\omega)\vec{E}(\omega) + \overset{\leftrightarrow}{\chi}^{(3)} \otimes \vec{E}(\omega)\vec{E}(\omega)\vec{E}(\omega) + \dots \quad (1)$$

The first term in Eq. (1) describes an ordinary linear polarization of the medium, while the second and the third terms are responsible for the generation of the second and third harmonics, correspondingly. In the scope of this work we are interested only in the third term, which is proportional to the third-order nonlinear optical susceptibility tensor  $\overset{\leftrightarrow}{\chi}^{(3)}$ . To calculate the intensity of third harmonic generated by a focused laser beam, one has to integrate Maxwell equations for the nonlinear wave at the frequency  $3\omega$  with the induced polarization term described by Eq. (1). We follow the procedure described in (Bjorklund, 1975) and use a slow varying amplitude equation to describe wave propaga-

tion along the  $z$ -axes, which is chosen to be perpendicular to the focal plane of the laser beam,

$$2ik_3 \frac{\partial E_3}{\partial z} + \nabla_T^2 E_3 = -\frac{\pi\omega_3^2}{c^2} \chi^{(3)} \frac{E_1^3}{(1+i2z/b)^3} \times \exp[-3k_1 r^2/b(1+i2z/b)] \times \exp[-i\Delta kz], \quad (2)$$

where  $E_1$  and  $E_3$  are the amplitudes of the incident fundamental field and third harmonic, respectively;  $k_1$  and  $k_3$  are the wave numbers for the pump and the TH beams, respectively;  $b = 2\pi\omega_0^2 n_1 / \lambda_1$  is the confocal parameter of the focused beam, where  $\omega_0$  is a spot size;  $\Delta k = (6\pi/\lambda)(n_3 - n_1)$  is the wave vector phase mismatch;  $\omega_3 = k_3 c$  and  $\chi^{(3)}$  is the nonlinear susceptibility of the medium. We assume a Gaussian profile for the focused beam. The existence of a nonlinear wave propagating only in one (forward) direction is the other assumption made in deriving Eq. (2). By integrating (2) across the interface, we obtain the amplitude for the electric field of the TH wave in the form:

$$E_3(r, z) = i \frac{3}{2} \frac{\pi\omega}{n_3 c} E_1^3 \frac{\exp\left[\frac{-3r^2}{\omega_0^2(1+i2z/b)}\right]}{1+i2z/b} \times \int_{z_0}^z \chi^{(3)} \frac{\exp[-i\Delta kz]}{(1+i2z/b)^2} dz, \quad (3)$$

The total TH power can be obtained by integrating the power density over the beam profile.

If there is a homogeneous medium in the focal plane of the laser beam, Eq. (3) produces a zero value for  $E_3$ , i.e., no third-harmonic signal will be detected (Boyd, 1992; Bjorklund, 1975). This result is generally explained in terms of the Gouy phase shift acquired by a focused laser beam. One can also use a theoretical approach utilizing Green function formalism (Cheng and Xie, 2002) to describe third harmonic generated by a tightly focused laser beam. The major difference is the use of a nonparaxial approximation in our approach, which is typically justified in the case of a moderate numerical aperture focusing objective (Jiang et al., 2000). The interface between two media results in an abrupt change of either the refractive index or the nonlinear susceptibility, or both, giving rise to a strong third-harmonic signal. Clearly the intensity of this signal is the function of the properties of the interface. Our goal is to extract the value of  $\chi^{(3)}$  for unknown medium. The easiest way to do it for solution is to use a covering glass medium as a reference medium, i.e., measure the third-harmonic signal generated on the interface between air and glass, and glass and unknown solution (see Fig. 1). This way there is no need in measuring the exact values of intensity and spot size of the incident laser beam, and scattering and absorption in solution will equally affect the intensity of both beams. The reflection from the first interface can be taken into account by introducing a

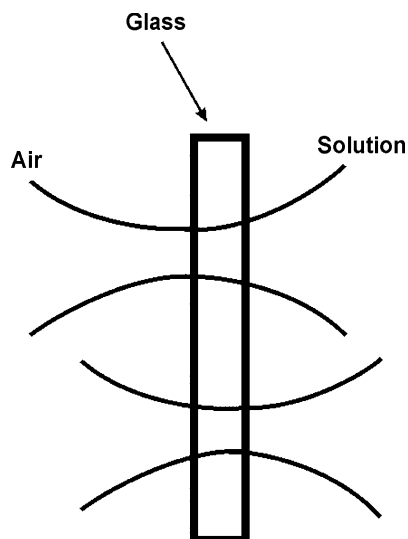


Fig. 1. A schematic diagram illustrating the ratio imaging scheme for  $\chi^{(3)}$  determination of unknown solution. The upper beam generates the third-harmonic signal on the air–glass interface, while the lower beam generates the signal on the glass–solution interface.

corrective coefficient, since in the above analysis the reflected wave is not considered. Assuming that aberration due to focusing are not important (which is true (Hell et al., 1993) for a moderate numerical aperture focusing lens in our experiments), the relative ratio of the third harmonics generated from two interfaces can be used to characterize the nonlinear susceptibility of unknown solution provided the prior knowledge of all the refractive indices and the nonlinear susceptibility of the covering glass.

From Eq. (3) we calculate the power of the third harmonic generated on each interface and take a ratio of these powers, making a relatively simple equation for a single unknown parameter,  $\chi^{(3)}$ , of unknown solution (Shcheslavskiy et al., 2003).

### 3. Experimental demonstration

To prove the validity of our approach we first use for our characterization a simple solution of methanol in water. As a cover glass we use a 170- $\mu\text{m}$ -thick fused silica window (Esco Products). The nonlinear optical susceptibility of fused silica in a nonresonant case is known:  $\chi_{\text{fused silica}}^{(3)} = 2.57 \times 10^{-14}$  esu. As a laser source we use a recently developed the long-cavity Cr:forsterite laser (Shcheslavskiy et al., 2001), which produces  $>200\text{-mW}$ , sub-40-fs, 1250-nm pulses at 26.5 MHz repetition rate. The choice of the wavelength is very appropriate for the variety of multiphoton microscopy applications, since laser light at 1250 nm does not scatter as much as the light at 800 nm (typical wavelength of femtosecond Ti:sapphire laser) allowing deeper penetration of laser radiation into the tissue (Tuchin, 2000; Golubovich

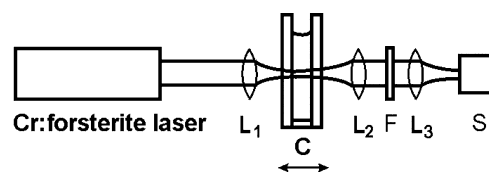


Fig. 2. A schematic of the experimental setup for  $\chi^{(3)}$  measurements. CS, a fused silica cover slip; F, a short-pass filter; S, a spectrometer with an attached liquid-nitrogen cooled CCD; MS, a microslide.

et al., 1997). In the same time both second and third harmonic of this radiation lie in a nonabsorbing spectral region, minimizing the possible damage. The laser beam is focused on the interface (see Fig. 2) by an aspheric lens ( $L_1$ ,  $f = 4.5$  mm,  $\text{NA} = 0.55$ ) and the third-harmonic radiation is collected by an aspheric lens ( $L_2$ ,  $f = 8$  mm,  $\text{NA} = 0.5$ ) and re-imaged with a lens ( $L_3$ ) into the spectrometer with an attached liquid-nitrogen-cooled CCD.

We use a water solution of methanol as a liquid, whose nonlinear optical susceptibility has to be determined. The choice is governed by the relatively well-known parameters of both liquids, so we can compare our measured results with the values measured by other techniques. Both methanol and water are transparent for the third harmonic, but we emphasize the fact that our method does not rely on the transparency of the sample, since the absorbing layer of a liquid will equally absorb the third-harmonic signals generated by both interfaces, and the signal level is at least 10 orders of magnitude above the detection limit of our system.

We mix methanol with the double-ionized distilled water and measure the third-harmonic power as a function of a relative methanol concentration. This dependence is shown in Fig. 3A. There is a very small difference in refractive indices of water ( $n_{\text{water}} = 1.326$ ) and methanol ( $n_{\text{methanol}} = 1.323$ ) at 1250 nm, while there is a dramatic change of the third-harmonic power for pure solutions of these liquids. The change of the third-harmonic power generated at the second interface is primarily due to the change of the nonlinear optical susceptibility of our solution.

We can determine the  $\chi^{(3)}$  values for solution (see Fig. 3B), and, knowing the exact concentration of liquids, the nonlinear susceptibilities of both liquids. It leads to the following values of nonlinear susceptibility for water and methanol:  $2.85 \times 10^{-14}$  and  $3.40 \times 10^{-14}$  esu, respectively. These values are in a very good agreement with the earlier published results (Kajzar and Messier, 1985).

### 4. Nonlinear susceptibility of ion-containing solutions

Many biological processes involve the variation of a local concentration of certain ions ( $\text{Ca}^{2+}$ ,  $\text{K}^+$ ,  $\text{Na}^+$ , etc.).

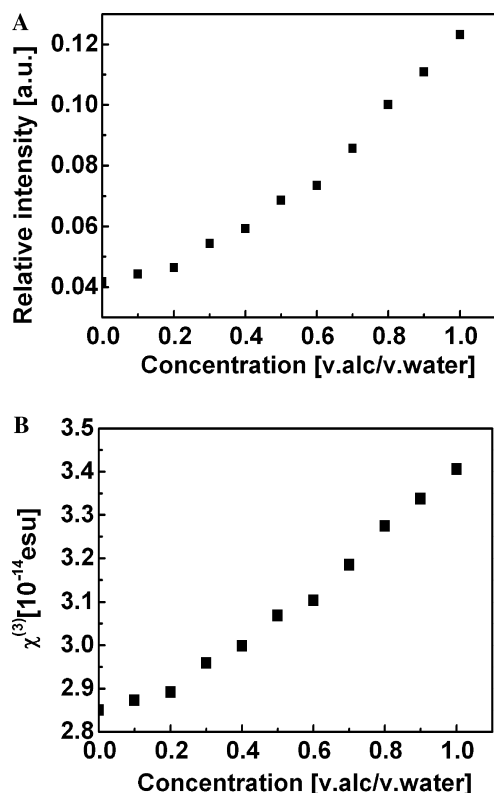


Fig. 3. (A) The ratio of the third-harmonic powers generated on two interfaces as a function of methanol concentration in water. (B) The measured value of  $\chi^{(3)}$  of solution as a function of methanol concentration in water.

To be able to explain and quantify results of microscopic third-harmonic imaging (Canioni et al., 2001), it is important to characterize a solution in terms of nonlinearity. As an illustrative example, we use a variable concentration of sodium chloride in the double ionized distilled water as a liquid, whose nonlinear optical susceptibility has to be measured. The results of these measurements are plotted in Fig. 4A as a function of the salt concentration. For the maximum concentration used in our experiments we observe as much as a fivefold increase of the relative third-harmonic power on the interface between solution and fused silica. There are no significant changes of the water refractive index as a function of salt concentration, and the above observation can be explained in terms of the increase of the third-order nonlinear optical susceptibility of the saline water solution. This increase of nonlinear optical susceptibility can be understood from a simple physical picture. When salt is added, sodium and chloride ions start to interact with different parts of the water molecule (oxygen and hydrogen, respectively), thus, stretching the molecule. This increases the dipole moment of the water molecule, the effect predicted by molecular dynamics simulations (Smith and Dang, 1994), and gives rise to a higher value of the nonlinear optical susceptibility. For the 30% sodium chloride water so-

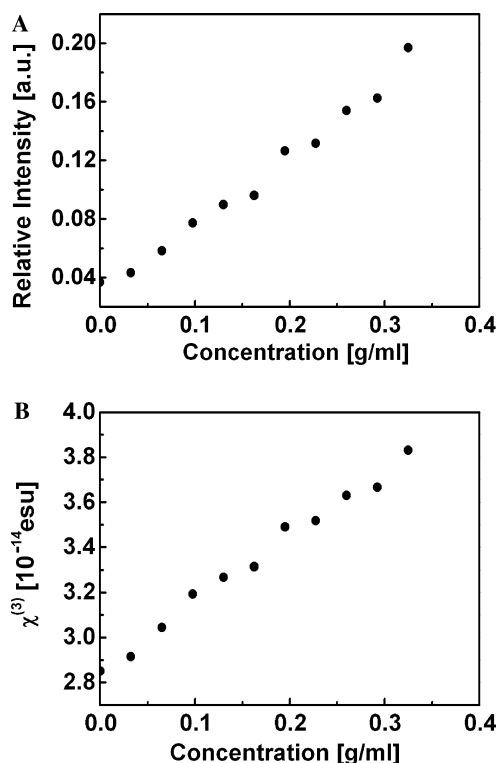


Fig. 4. (A) The ratio of the third-harmonic powers generated on two interfaces as a function of sodium chloride concentration in distilled water. (B) The measured value of  $\chi^{(3)}$  of solution as a function of sodium chloride concentration in distilled water.

lution we obtain the value of  $\chi^{(3)}$  to be  $3.69 \times 10^{-14}$  esu. Since the signal intensity is not directly related to the absolute value of this nonlinearity, but rather depends on the difference of two nonlinearities, which is typically much smaller than the absolute value by itself, the resulted changes in the third harmonic are significantly larger than the changes in the nonlinearity of the solution. It gives us a promise that third-harmonic imaging microscopy may become a valuable tool for monitoring dynamic changes of local ionic concentration (Canioni et al., 2001). However, some prior knowledge is required since the third-harmonic generation process does not distinguish between different ions and is sensitive rather to the changes of polarization of molecules induced by the variation of local concentration of these ions.

## 5. Structural changes in collagen

Collagen, being one of the most important proteins in living organism (Karp, 2002), was studied primarily by second harmonic imaging technique (Tuchin, 2000; Guo et al., 1996; Stoller et al., 2002; Kim et al., 1999). Collagen molecule has a triple-helix structure, which consists of three polypeptide chains coiled into a left

handed helix. Three left-handed chains then intervene to form a superhelix. Its rod-like structure has a diameter of about 1.4 nm and the length of about 300 nm. There are about 17 types of collagen, but the most widespread is type I collagen, which is the major structural component of skin, bone, dentin and other connective tissues in which it exists in forms of fibrils with diameters from 30 to 300 nm. The molecular weight of this biopolymer is about 300 kDa, and consequently the molecular weight of a collagen monomer is 100 Da.

In spite of the fact that there was a comprehensive study on collagen, which allowed to determine orientational order of collagen in tissues, second-order of nonlinear susceptibility of fibrils and other important properties of this protein many questions were left unanswered.

What is the relationship between the structure of collagen and its nonlinear optical properties? What are the first- and second-order hyperpolarizabilities of collagen in monomer form? It is important to know that to better understand structural changes which can happen during processes of thermal denaturation, glycation, enzymatic cleavage, and other processes, which are specific for pathophysiologic conditions in biological tissues. Comparison of the results on nonlinear susceptibility of the collagen at different levels of organization (monomer-fibril-fascicle) may provide very important information on polarity of the biological tissues in general.

All the nonlinear optical studies of collagen have been performed with either the biological tissues, containing collagen fibrils, or with fascicles deposited on the slides. In first case, there are a lot of other factors influencing second harmonic generation (for instance, elastin can contribute to second harmonic generation from skin). In the latter case, measurements were done at the conditions far from physiological conditions.

This paper we present the first results on measurements of second-order hyperpolarizability of collagen trimers. To the best of our knowledge such measurements are done for the first time.

Collagen type I is obtained from calf skin and supplied by ICN Biomedicals. Following the recipe (Kaminska and Sionkowska, 1996), we dissolve the protein in 0.04 M acetic acid solution with a concentration of about 10 mg/ml. Then this concentrate is used for adding to pure 0.04 M acetic acid solution in experiment. The pH of the solution is 4.8.

The relative power of the third harmonic is shown in Fig. 5A as a function of collagen's concentration. We can determine the  $\chi^{(3)}$  values for collagen solution using equation for normalized third-harmonic signal and using the known value of  $\chi^{(3)}$  values for fused silica. The third-order nonlinear susceptibility of the solution can be written as (Verbiest et al., 1994):

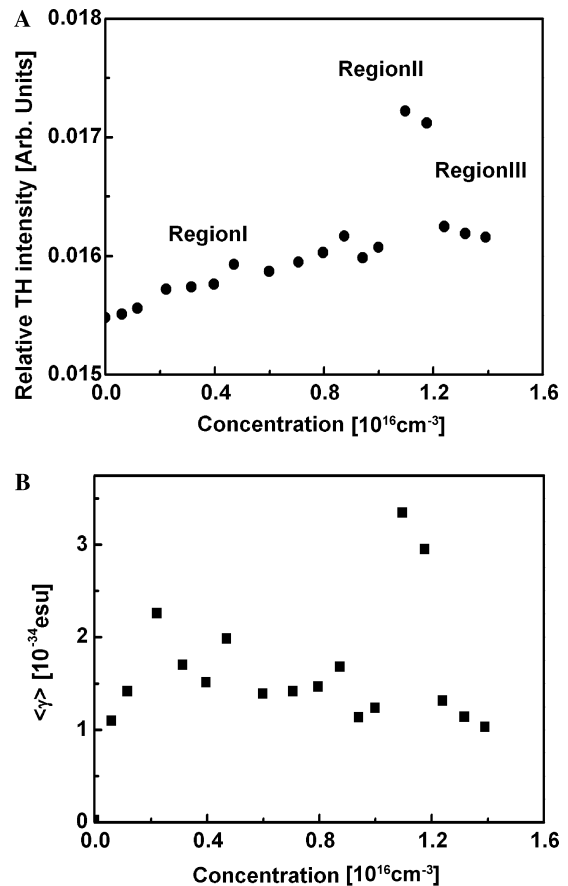


Fig. 5. (A) The ratio of the third-harmonic powers generated on two interfaces as a function of collagen molecules' concentration in solution. (B) The measured value of second-order hyperpolarizability  $\langle \gamma \rangle_{\text{col}}$  as a function of collagen molecules' concentration in solution.

$$\chi_{\text{sol}}^{(3)} = F^4 \times [N_{\text{col}} \langle \gamma \rangle_{\text{col}} + N_{\text{acid}} \langle \gamma \rangle_{\text{acid}}], \quad (4)$$

where  $F$  is the local field correction factor:  $F = (n^2 + 2)/3$ ;  $N_{\text{col}}$ ,  $N_{\text{acid}}$  are the number of collagen and water molecules, respectively;  $\langle \gamma \rangle_{\text{col}}$  and  $\langle \gamma \rangle_{\text{acid}}$  represent the orientationally averaged second-order hyperpolarizability of collagen and acetic acid molecules, respectively.

From the concentration dependence of  $\chi^{(3)}$  for the collagen solution we determine  $\langle \gamma \rangle_{\text{col}}$  from Eq. (4) (see Fig. 5B). In the analysis of these measurements we make the assumption that the local field correction factors are independent of the molecular species, and that refractive index is independent on concentration in these relatively dilute solutions. At concentrations up to 5.5 mg/ml ( $10^{16}$  collagen molecules per  $\text{cm}^3$ ): Region I, we get  $\langle \gamma \rangle_{\text{col}} \cong 1.5210^{-34} \text{esu}$ .

At concentrations of collagen 5.6 mg/ml, which corresponds to  $1.05 \times 10^{16}$  collagen molecules per  $\text{cm}^3$  in solution, we observe a rapid increase of the relative third-harmonic signal (see Fig. 5A, Region II). In terms of the second-order hyperpolarizability of collagen, it

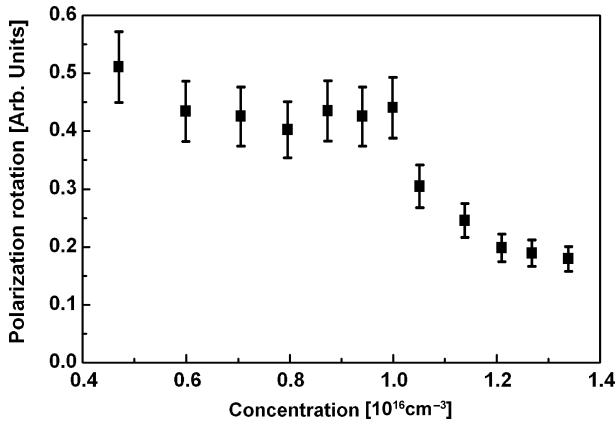


Fig. 6. The angle of polarization rotation of collagen in solution as a function of collagen molecules' concentration in solution.

increases nearly twice in comparison to the Region I, and amounts to  $3.34 \times 10^{-34}$ esu (at 5.6 mg/ml). Such strong enhancement of hyperpolarizability can be possible in the case when there are strong local inhomogeneities in solution. We should note that this aggregated collagen is a polar material since the nonlinear hyperpolarizability is increased (Prasad and Williams, 1991).

After increase of third-harmonic signal we observe a rather fast decrease in the signal and, correspondingly, in second-order hyperpolarizability (Region III in Figs. 5A and B). The possible reason for this drop is that at high concentrations of collagen a process similar to helix–coil transition happens and as a consequence a structural order is destroyed which brings to the drop of the harmonic signal (Kaminska and Sionkowska, 1996).

In order to verify our later hypothesis we also measure the circular dichroism of collagen solution. We find that in earlier identified Region III the collagen solution experiences significant reduction of the circular dichroism (the angle of rotation per unit concentration decreases by a factor of three with respect to original value (see Fig. 6). This finding confirms our original assumption of the transformation behavior of collagen observed by the third-harmonic generation.

### 6. Imaging of small nanostructures

So far we have considered the third-harmonic generation on the interface of only two media. What happens if a small object (with the size much smaller than the Rayleigh length of the focused laser beam) is placed in the focal plane? Will it produce the third-harmonic signal and how strong this signal will be?

For simplicity, we consider a cylindrical object of the radius  $R$  and the length  $2R$  placed symmetrically with respect to the focal plane of the laser beam (see Fig. 7). In this case the integration in Eq. (3) along  $z$ -axis results in three separate integrals:

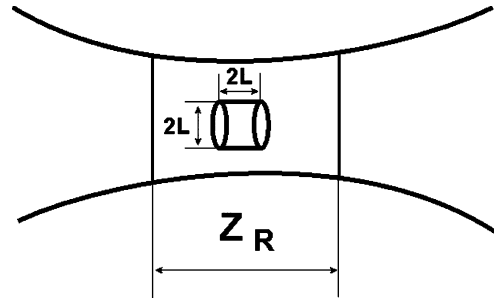


Fig. 7. A schematic diagram illustrating application of the third-harmonic generation to the detection of ultra-small particles in solution.  $Z_R$  is the Rayleigh length,  $R$  is the characteristic size of a particle.

$$P_v \propto \left| \gamma_{\text{water}} \int_{-\infty}^{-R} \frac{\text{Exp}[-i\Delta k_w z]}{(1 + 2iz/b)^2} dz + \gamma_{\text{mat}} \int_{-R}^R \frac{\text{Exp}[-i\Delta k_c z]}{(1 + 2iz/b)^2} dz + \gamma_{\text{water}} \int_R^{\infty} \frac{\text{Exp}[-i\Delta k_w z]}{(1 + 2iz/b)^2} dz \right|^2, \quad (5)$$

where  $\gamma_{\text{mat}}$  is the hyperpolarizability of material of these cylinders. Integrating Eq. (5), results in the fourth power dependence of the generated third-harmonic signal on the characteristic size of a microscopic object,  $R$  (Shcheslavskiy et al., 2003).

We experimentally test this dependence by measuring the power of the third harmonic generated in the volume of the liquid, when small polystyrene beads (Polysciences) are placed in the water solution, which was flowing through a cell to avoid possible trapping of microspheres by a laser beam. A typical dependence of the third-harmonic power on the concentration of these

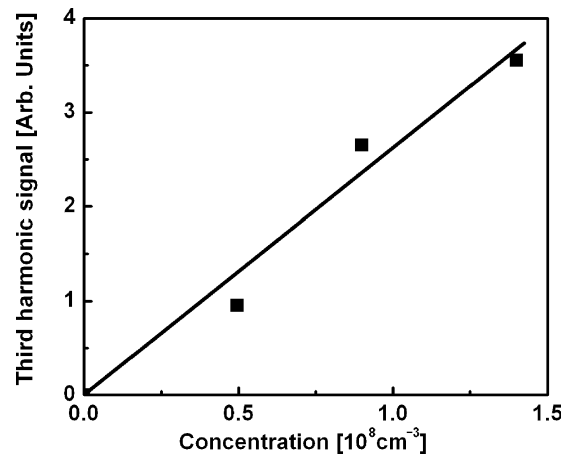


Fig. 8. The measured power of the third-harmonic signal generated in the bulk of solution containing 700-nm size polystyrene microspheres as a function of microspheres' concentration. Squares—experimentally measured data points, solid guide is drawn to provide a guide to an eye.

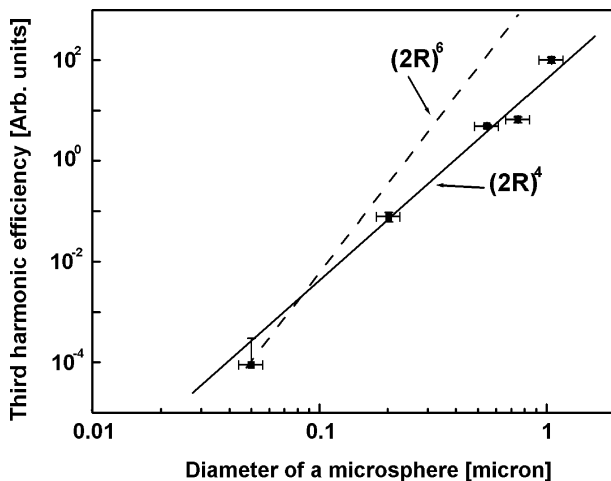


Fig. 9. The power of the third-harmonic signal generated in the bulk of solution containing polystyrene microspheres as a function of microspheres' size. Squares—experimentally measured data points, solid guide shows a fourth power dependence, dashed line shows for comparison a sixth power dependence.

microspheres is shown in Fig. 8. Clearly, the third-harmonic signal is rather strong and detectable even for the lowest concentrations of microspheres. These results can be expressed in terms of the signal per microparticle, which shows a fourth power dependence on the size of microspheres (see Fig. 9). The power of the third-harmonic signal even for the smallest size spheres (50 nm) scaled per one particle is still above the sensitivity level of a typical photon counting PMT, i.e. even smaller (down to 20–30 nm) particles incorporated in a homogeneous medium could be detected. The ability to see these nanostructures may find application in correlated spectroscopy based on the third-harmonic imaging (Faustov et al., 2003), which compared to a commonly used fluorescence correlation spectroscopy (see, for example, (Korlach et al., 1999)) utilizes a natural ability of any micro- and nanostructure to generate light at the frequency of the third harmonic.

## 7. Conclusion

In summary, we have demonstrated that third-harmonic generation may serve as an invaluable tool for microscopic imaging. While the third-harmonic signal vanishes in a homogeneous medium, it arises in biological tissues, which possess a variety of interfaces, and can be a source of valuable information on the structure of interfaces and solution on both sides of an interface. The inhomogeneities *inside* the cell, which lead to the nonvanishing third-harmonic signal, can be also in the form of a local variation of ionic concentration (for example,  $\text{Ca}^{2+}$ ) and can be detected and characterized noninvasively by means of the third-harmonic micros-

copy. An ability to noninvasively detect micro- and nanostructures inside cells, and structural sensitivity of the third harmonic may be used for gaining important information about biological structures and their hierarchy. In the same time, relatively strong signals make it possible real-time observations and dynamic measurements of the changes on the micro- and nanolevel.

## Acknowledgments

This work is partially supported by NATO Grant CLG-979419, NSF Grants ECS-9984225, and NIH Grants R21RR14257, R21RR16282, and R15CA83910. Vladislav Shcheslavskiy acknowledges the University of Wisconsin—Milwaukee Graduate School Fellowship.

## References

- Barad, Y., Eisenberg, H., Horowitz, M., Silberberg, Y., 1997. Nonlinear laser scanning microscopy by third-harmonic generation. *Appl. Phys. Lett.* 70, 922–924.
- Bjorklund, G., 1975. Effects of focusing on third-order nonlinear processes in isotropic media. *IEEE J. Quantum Electron.* 11, 287–296.
- Boyd, R.W., 1992. *Nonlinear optics*, third ed. Academic Press, Boston.
- Campagnola, P.J., Millard, A.C., Terasaki, M., Hoppe, P.E., Malone, C.J., Mohler, W.A., 2002. Three-dimensional high resolution second-harmonic generation imaging of endogenous proteins in biological tissues. *Biophys. J.* 81, 493–508.
- Canioni, L., Rivet, S., Sarger, L., Bariller, R., Vacher, P., Voisin, P., 2001. Imaging of  $\text{Ca}^{2+}$  intracellular dynamics with a third-harmonic microscope. *Opt. Lett.* 26, 515–517.
- Cheng, J.-X., Xie, X.S., 2002. Green's function formulation for third-harmonic generation microscopy. *J. Opt. Soc. Am. B* 19, 1604–1610.
- Delfino, M., 1978. A comprehensive optical second harmonic generation study of the non-centrosymmetric character of biological structures. *J. Biol. Phys.* 6, 105–117.
- Denk, W., Strickler, H., Webb, W.W., 1990. 2-photon laser scanning fluorescence microscopy. *Science* 248, 73–76.
- Duncan, M.D., Reintjes, J., Manuccia, T.J., 1982. Scanning coherent anti-Stokes Raman microscope. *Opt. Lett.* 7, 350–352.
- Faustov, A.R., Shcheslavskiy, V., Petrov, G.I., Yakovlev, V.V., 2003. Third-harmonic correlation spectroscopy. To be published.
- Freund, I., Deutsch, M., Sprecher, A., 1986. Optical second-harmonic microscopy, crossed-beam summation, and small-angle scattering in rat-tail tendon. *Biophys. J.* 50, 693–712.
- Golubovich, B., Bouma, B.E., Tearney, G.J., Fujimoto, J.G., 1997. Optical frequency-domain reflectometry using rapid wavelength tuning of a  $\text{Cr}^{4+}$ :forsterite laser. *Opt. Lett.* 22, 1704–1706.
- Guo, Y., Ho, P.P., Tirkslinas, A., Liu, F., Alfano, R.R., 1996. Optical harmonics generation from animal tissues by use of picosecond and femtosecond laser sources. *Appl. Opt.* 35, 6810–6813.
- Hell, S.W., Reiner, G., Cremer, C., Stelzer, E.H.K., 1993. Aberrations in confocal fluorescence microscopy induced by mismatches in refractive index. *J. Microsc.* 169, 391–405.
- Jiang, Y., Jakubczyk, D., Shen, Y., Prasad, P.N., 2000. Nanoscale nonlinear optical processes: theoretical modeling of second-harmonic generation for both forbidden and allowed light. *Opt. Lett.* 25, 640–642.

- Kajzar, F., Messier, J., 1985. Third-harmonic generation in liquids. *Phys. Rev. A* 32, 2352–2363.
- Kaminska, A., Sionkowska, A., 1996. Effect of UV radiation on the infrared spectra of collagen. *Polym. Degrad. Stabil.* 51, 19–26.
- Karp, G., 2002. *Cell and Molecular Biology*, third ed. John Wiley and Sons.
- Kim, B., Eichler, J., Da Silva, L.B., 1999. Frequency doubling of ultrashort laser pulses in biological tissues. *Appl. Opt.* 38, 7145–7150.
- Korlach, J., Schwille, P., Webb, W.W., Feigenson, G.W., 1999. Characterization of lipid bilayer phases by confocal microscopy and fluorescence correlation spectroscopy. *Proc. Natl. Acad. Sci. USA* 96, 8461–8466.
- Müller, M., Squier, J., Wilson, K.R., Brakenhoff, G.J., 1998. 3D microscopy of transparent objects using third-harmonic generation. *J. Microsc.* 191, 266–274.
- Moreaux, L., Sandre, O., Charpak, S., Blanchard-Desce, M., Mertz, J., 2001. Coherent scattering in multi-harmonic light microscopy. *Biophys. J.* 80, 1568–1574.
- Peleg, G., Lewis, A., Linial, M., Loew, L.M., 1999. Nonlinear optical measurement of membrane potential around single molecules at selected cellular sites. *Proc. Natl. Acad. Sci. USA* 96, 6700–6704.
- Petrov, G.I., Saltiel, S., Minkovski, N., Heathcote, R.D., Yakovlev, V.V., 2003. Nonlinear optical imaging of membrane structures. *Laser Physics Letters* 1, 10–15.
- Potma, E.O., de Boeij, W.P., Wiersma, D.A., 2000. Nonlinear coherent four-wave mixing in optical microscopy. *J. Opt. Soc. Am. B* 17, 1678–1684.
- Prasad, N., Williams, D., 1991. *Introduction to Nonlinear Optical Effects in Molecules and Polymers*. John Wiley & Sons, New York.
- Shcheslavskiy, V., Yakovlev, V.V., Ivanov, A.A., 2001. High-energy self-starting femtosecond Cr<sup>4+</sup>:Mg<sub>2</sub>SiO<sub>4</sub> oscillator operating at a low repetition rate. *Opt. Lett.* 26, 1999–2001.
- Shcheslavskiy, V., Petrov, G., Yakovlev, V.V., 2003. Nonlinear susceptibility measurements of solutions using third-harmonic generation on the interface. *Appl. Phys. Lett.* 82, 3982–3984.
- Shcheslavskiy, V., Petrov, G.I., Saltiel, S., Yakovlev, V.V., 2003. Third-harmonic generation from microspheres. To be published.
- Shen, Y.R., 1996. A few selected applications of surface nonlinear optical spectroscopy. *Proc. Natl. Acad. Sci. USA* 93, 12104–12108.
- Smith, D.E., Dang, L.X., 1994. Computer-simulations of NaCl association in polarizable water. *J. Chem. Phys.* 100, 3757–3766.
- Squier, J., Muller, M., Brakenhoff, G., Wilson, K., 1998. Third harmonic generation microscopy. *Opt. Express* 3, 315–324.
- Stoller, P., Reiser, K., Celliers, P., Rubenchik, M., 2002. Polarization-modulated second harmonic generation in collagen. *Biophys. J.* 82, 3330–3342.
- Tuchin, V., 2000. *Tissue Optics*. SPIE Press, Bellingham, WA.
- Verbiest, T., Kauranen, M., Persoons, A., Ikonen, M., Kurkela, J., Lemmetyinen, H., 1994. Nonlinear optical activity and biomolecular chirality. *J. Am. Chem. Soc.* 116, 9203–9205.
- Yakovlev, V.V., Govorkov, S.V., 2001. Diagnostics of surface layer disordering using optical third harmonic generation of a circular polarized light. *Appl. Phys. Lett.* 79, 4136–4138.
- Yelin, D., Silberberg, Y., 1999. Laser scanning third-harmonic-generation microscopy in biology. *Opt. Express* 5, 169–175.
- Zhang, J., Davidson, R.M., Wei, M.D., Loew, L.M., 1998. Membrane electric properties by combined patch clamp and fluorescence imaging in single neurons. *Biophys. J.* 74, 48–53.
- Zumbusch, A., Holton, G.R., Xie, X.S., 1999. Three-dimensional vibrational imaging by coherent anti-stokes Raman scattering. *Phys. Rev. Lett.* 82, 4142–4145.